Numerical Simulation of Atmosphere-Ocean-Sea Ice Interaction During Interannual Cycle in High Northern Latitudes*

LIU Xiying[1†](刘喜迎), LIU Hailong[1](刘海龙), LI Wei[1](李 薇), ZHANG Xuehong[1](张学洪), YU Rucong[2] (宇如聪), and YU Yongqiang[1](俞永强)

1 *LASG, Institute of Atmospheric Physics, Chinese Academy of Sciences, Beijing* 100029
2 *China Meteorological Administration, Beijing* 100081

(Received December 3, 2007)

ABSTRACT

The interannual atmosphere-ocean-sea ice interaction (AOSI) in high northern latitudes is studied with a global atmosphere-ocean-sea ice coupled model system, in which the model components of atmosphere and land surface are from China National Climate Center and that of ocean and sea ice are from LASG, Institute of Atmospheric Physics, Chinese Academy of Sciences. A daily flux anomaly correction scheme is employed to couple the atmosphere model and the ocean model with the effect of inhomogenity of sea ice in high latitudes is considered. The coupled model system has been run for 50 yr and the results of the last 30 years are analyzed. After the sea level pressure (SLP), surface air temperature (SAT), sea surface temperature (SST), sea ice concentration (SIC), and sea surface sensible heat flux (SHF) are filtered with a digital filter firstly, their normalized anomalies are used to perform the decomposition of combined complex empirical orthogonal function (CCEOF) and then they are reconstructed with the leading mode. The atmosphere-ocean-sea ice interactions in high northern latitudes during a periodical cycle (approximately 4 yr) are analyzed. It is shown that: (1) When the North Atlantic Oscillation (NAO) is in its positive phase, the southerly anomaly appears in the Greenland Sea, SAT increases, the sea loses less SHF, SST increases and SIC decreases accordingly; when the NAO is in its negative phase, the northerly anomaly appears in the Greenland Sea, SAT decreases, the sea loses more SHF, SST decreases and SIC increases accordingly. There are similar features in the Barents Sea, but the phase of evolution in the Barents Sea is different from that in the Greenland Sea. (2) For an average of multi-years, there is a cold center in the inner part of the Arctic Ocean near the North Pole. When there is an anomaly of low pressure, which is closer to the Pacific Ocean, in the inner part of the Arctic Ocean, anomalies of warm advection appear in the region near the Pacific Ocean and anomalies of cold advection appear in the region near the Atlantic Ocean. Accompanying with these anomalies of warm and cold advection in these two regions, warm and cold anomalies appear respectively. Accordingly, SHF sent to the atmosphere from the sea surface decreases and increases, and SST increases and decreases, SIC decreases and increases in these two regions. When there is an anomaly of high pressure in the inner part of the Arctic Ocean, the former relationships reverse. From these results, it can be deduced that, during the interannual cycle of the coupled atmosphere-ocean system, the variability of large-scale atmospheric circulation plays a dominant role and variations of SST and SIC are mainly responding to that of atmospheric circulation.

Key words: coupled model, atmosphere-ocean-sea ice interaction (AOSI), combined complex empirical orthogonal function (CCEOF)

1. Introduction

In recent years, the climate in northern polar region has been given more attentions with the increase of accumulated observation data and the improvement of data quality. Especially, people are trying to discern signals of climate change due to human activities from the background of natural variability in the global atmosphere-ocean-sea ice coupled system. With the advent of practical use of the remotely-sensed sea ice data retrieved from microwave sensors onboard satellite after October 1978, the temporal continuity of observation data is improved and the spatial coverage of observation data is expanded, so that more valuable data are feasible for research on physical processes connected with sea ice, and the research on AOSI can

*Supported jointly by the National Natural Science Foundation of China under Grant No. 40675065 and National Basic Research Priorities Program of China under Grant No. 2005CB32170X.
†Corresponding author: liuxy@lasg.iap.ac.cn.

be triggered effectively.

At present, researches on AOSI concern a broad scope, in which some concentrate on local or regional scales and some concentrate on larger spatial scales such as semi-hemisphere or the whole globe. The main methods are to seek relationships between fields in observed data (Agnew, 1993; Jiang et al., 1996; Gao and Wu, 1998) or to explore atmospheric responses to sea ice anomalies with numerical experiments (Huang and Yang, 1992; Ni et al., 1992; Honda et al., 1999). The research based on the analysis of observation data can be impeded by data availability, and the numerical experiments of sea ice forcing the atmosphere can only depict the mechanism of forcing and response. Since numerical coupled model is a kind of simplification of the real climate system and the physical processes of AOSI are considered, it is of special advantages to study AOSI. Based on the analysis of observation data, it is shown that the features of interaction between atmosphere and ocean are related to temporal scales. On interannual scales, though there are still debates to some extent, most researchers believe that the variations of sea ice are due to the variability of atmospheric large-scale general circulation (Slonosky et al., 1997; Wu et al., 2000; Liu et al., 2005) with no elimination that variations of atmospheric circulation in local area are responses to that of sea ice cover (Deser et al., 2000). In studies of AOSI based on observation data, since the data employed come from different spheres of the climate system with different observation errors and the consistencies in dynamics and thermodynamics between them are not guaranteed, the real features of AOSI may be concealed by these faults and correct results may not be achieved at times. By contrast, in researches with coupled numerical model, the consistencies of physical fields in model results are guaranteed by given formula. But the reliability of model outputs may arise other problems. At present, research results on AOSI with coupled model are less.

In the work, the simulation results, such as SLP, SAT, SST, SIC, and SHF of a global coupled atmosphere-ocean-sea ice model are used to perform the decomposition of CCEOF and then they are reconstructed with the leading mode. The variations and their connections during a periodical cycle (the period is approximately 4 yr) in the reconstructed physical fields are analyzed and the features of AOSI in the interannual cycle are discussed.

2. Model and analysis method

2.1 Model

The atmospheric general circulation model (AGCM) component of the coupled model comes from China National Climate Center (Ye et al., 2000). The AGCM is a spectral model of triangular truncation with 63 wave numbers (approximately 1.875°×1.875°) for fields in the horizontal. A hybrid coordinate is used in the vertical and all variables except vertical velocity situates on full levels (the top and bottom boundaries of the model atmosphere are designated half levels). For the vertical coordinate, it is a common σ-coordinate near the ground, a p-coordinate in the stratosphere, and a form of hybrid elsewhere. The model atmosphere is divided into 16 layers with 4 layers within the planetary boundary layer. There is a simple land surface model contained in the AGCM.

The oceanic general circulation model (OGCM) component of the coupled model is T63L30, which is a version of the world ocean general circulation model in the Institute of Atmospheric Physics, Chinese Academy of Sciences (Jin et al., 1999). The OGCM is a baroclinic model using geographical spherical coordinates with static balance and Boussinesq approximation employed and has a horizontal resolution nearly equal to that of the AGCM (approximately 1.875°×1.875°). The model's top boundary is a free surface (Zhang et al., 1996). An η-coordinate is adopted in the vertical and the model ocean is divided into 30 layers unevenly with 12 layers within the 300-m upper. The model variables are allocated with Arakawa B grid. A thermodynamic sea ice model with schemes similar to Semnter (1976) and Parkinson and Washington (1979) is used to simulate the distribution of sea ice concentration, sea ice thickness, and sea ice surface temperature. The OGCM has once been used to couple with another sea ice model with both

thermodynamic and dynamic processes considered (Liu et al., 2000).

Grotzner et al. (1996) and Liu et al. (2004) employed a flux aggregation scheme to represent the effect of sea ice inhomogeneities on flux exchange, a modified daily flux anomaly coupling scheme (Yu and Zhang, 2000) is used to realize the coupling of the AGCM with the OGCM under the consideration of sea ice inhomogeneities in high latitudes. A 50-yr coupled model integration has been achieved but only the last 30-yr results will be used in the following analysis to exclude the influence of model spin-up.

2.2 Analysis method

To pick out signals of interannual variations, some physical variables are processed with a digital filter at first. The filter is constructed as follows:

$$Y_t = \sum_{k=-K}^{K} a_k X_{t+k}, \tag{1}$$

where $\{a_{-K}, \ldots, a_K\}$ are weight coefficients, totally real numbers $2K+1$, and $a_{-K} = a_K$. K takes 48 in the work, and the values of $a_0, \ldots, a_{48}$ are listed in Table 1.

From the response function of frequency for the filter (figure omitted), only signals of 3–5 yr are retained.

The filtered physical variables are normalized and their normalized anomalies are used to perform the decomposition of CCEOF. The decomposed fields are then reconstructed with the leading mode. The aim of performing combined decomposition here for several fields is to ensure that they have identical initial phases so as to make it easy to analyze the combined variability of those anomalies varying concurrently. Complex empirical orthogonal function (CEOF) decomposition, also known as the Hilbert empirical orthogonal function (EOF) method, can detect features of propagation in the analyzed data besides keeping the merits of traditional EOF decomposition. The reader can refer to references (Barnet, 1983; Horel, 1984) for details of CEOF decomposition. A brief description will be outlined here only. For a given temporal series, its complex counterpart is constructed by Hilbert transformation, which can give information of temporal change rate at a certain moment for the initial series, with its real part being the original series and its imaginary part being the result of Hilbert transformation on the original one. Then EOF decomposition is performed for the complex series. The eigenvectors and temporal coefficients of decomposition results, which are complex, can be used to reconstruct a field with leading modes as in the traditional EOF analysis. Usually, the real part of the reconstructed field is analyzed only.

Table 1. Weight coefficients of digital filter

Ones position	Tens position				
	0	1	2	3	4
0	0.022222	0.003781	−.019227	−.009189	0.010684
1	0.022001	0.000757	−.019842	−.006792	0.013040
2	0.021344	−.002256	−.020053	−.004326	0.013771
3	0.020264	−.005193	−.019862	−.001842	0.014197
4	0.018784	−.007997	−.019282	0.000606	0.014319
5	0.016937	−.010610	−.018331	0.002968	0.014147
6	0.014761	−.012981	−.017036	0.005197	0.013697
7	0.012303	−.015064	−.015432	0.007250	0.012989
8	0.009615	−.016818	−.013559	0.009090	0.012050
9	0.006755	−.018214	−.011462	0.010684	

The method for approximation of Hilbert transformation for finite temporal series in the work is illustrated as follows:

The temporal series x_t can be approximately expressed by Fourier expansion:

$$x_t = \sum_k \left[a_k \cos\left(\frac{2\pi kt}{n}\right) + b_k \sin\left(\frac{2\pi kt}{n}\right) \right], \tag{2}$$

and its Hilbert transformation $\hat{x}_t^H$ can be estimated by

$$\hat{x}_t^H = \sum_k \left[b_k \cos\left(\frac{2\pi kt}{n}\right) - a_k \sin\left(\frac{2\pi kt}{n}\right) \right]. \quad (3)$$

The monthly anomalies of SLP, SAT (denoted by air temperature on the lowest model layer), SST, IC, and SHF are calculated at first, and then these anomalies are processed by the band pass filtering technique as mentioned above to extract interannual signals. The filtered fields are normalized and then decomposed by CCEOF. Subsequently, the physical fields are reconstructed with the leading mode which represents 32% of the total variance. The feature of phase variation of the temporal coefficient corresponding to the leading mode is that the phase varies from 360° to 0° repeatedly with time. Within a range of 360°, the phase decreases quasi-linearly and the variation spans about 4 yr, representing that the combined variation of SLP, SAT, SST, SIC, and SHF has a period of nearly 4 yr. Eight phases, e.g., 360°, 315°, 270°, 225°, 180°, 135°, 90°, and 45°, are selected and composites of these phases are made for the five reconstructed anomalies. The time span of two neighboring phases is about half a year. Based on results of composites made by methods mentioned above, the features of interannual cycle in the modeled atmosphere-ocean (including sea ice) and their interactions will be analyzed.

3. Interannual cycles in the atmosphere, oceans and their interactions

3.1 Interannual cycle in the atmosphere

As shown in Fig.1, which are composites corresponding to eight phases of reconstructed SLP, the most prominent feature in SLP anomalies is the destruction and reconstruction of zonal symmetry properties and the transition between positive and negative phases of NAO. In the 0th year, most regions in the high northern latitudes are covered by positive anomalies of SLP whereas other part southward by negative anomalies. The obvious feature of zonal symmetry in SLP anomalies resembles Arctic Oscillation (AO). Subsequently, the area covered with negative anomalies in eastern Siberia extends and moves towards the central Arctic Ocean. In the 0.5th year, the central Arctic Ocean has been partly covered by negative anomalies. Meanwhile, the NAO is in its negative phase. In the 2nd year, the area covered by negative anomalies reaches its maximum and is surrounded by the positive anomaly areas. The circulation pattern of anomalies is contrary to that in the 0th year and the feature of zonal symmetry reestablishes. In the 2.5th year, the area covered with positive anomalies in eastern Siberia extends and moves towards the center of the Arctic Ocean and the NAO is in its positive phase. In the 3rd year, the central Arctic Ocean is mostly covered with positive anomalies, which extends later and reaches its maximum in the 4th (0th) year. Then, a new cycle repeats.

As shown in Fig.2 which are composites corresponding to eight phases of reconstructed SAT, there is an inverse tendency of variation between SAT in the Beaufort Sea and the Chukchi Sea and that in other regions within the Arctic Ocean. During the 0th–1.5th year, there is a negative anomaly of SAT in the Beaufort Sea and the Chukchi Sea and a positive anomaly of SAT in other regions, whereas during the 2nd–3.5th year, the cases reverse. This kind of inverse tendency of variation in SAT is connected with the changes of atmospheric general circulation in Fig.1. In the 0th year, the Greenland Sea is covered with the positive anomaly of SAT and the Barents Sea is partly covered with the negative anomalies. Half a year later, the Barents Sea is totally covered with negative anomalies and the area covered with positive anomalies in the Greenland Sea reduces. Later on, the area covered with negative anomaly in the Greenland Sea extends and occupies the whole region of the Greenland Sea in the 2nd year. Meanwhile, part of the Barents Sea, which was covered with negative anomaly, is now covered with positive anomalies. Later on, the area covered with positive anomalies extends and moves and then occupies the whole region of the Greenland Sea in the 3.5th year while the Barents Sea has been partly covered with negative anomalies. Afterwards, a new cycle repeats.

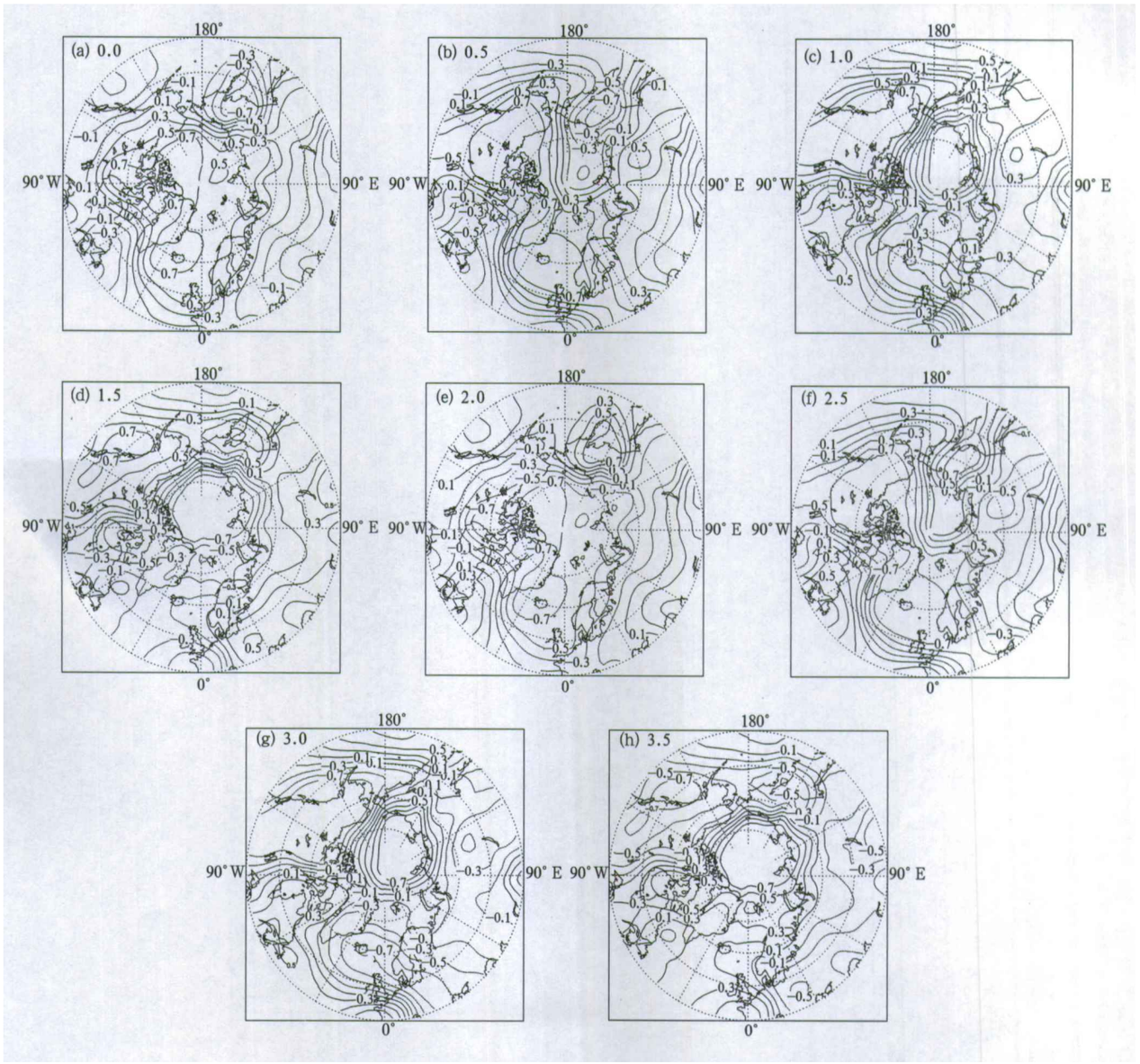

Fig.1. Composites of reconstructed sea level pressure (SLP) for eight phases. The number below each panel represents the corresponding phase within a cycle (approximately 4 yr).

3.2 Interannual cycle in the ocean

The composites corresponding to eight phases of reconstructed SST is shown in Fig.3. It can be seen that there is a phenomenon of anticlockwise propagation of SST anomalies within the Arctic Ocean, which is connected with the movement of anomaly center of atmospheric general circulation. In the 0th year, the center of positive anomaly within the Arctic Ocean is near 90°E. Later, the anomaly moves anticlockwise. It moves to the place near 120°W in the 2nd year and to the place near 60°E in the 3.5th year. Then, a new cycle repeats (4th year=0th year). Accompanying with the anticlockwise movement of positive anomaly, an area of negative anomaly, whose center is near 120°W in the 0th year, propagates anticlockwise also. The inner part of the Arctic Ocean is covered by a pair of anomalies totally. The SST anomaly in the Greenland Sea, Barents Sea, and Norway Sea exhibits stationary oscillations, with positive phase in the 2.0th–2.5th year, negative phase in the 0th–0.5th year and transition period in the 1st and 3rd year. The sign of SST

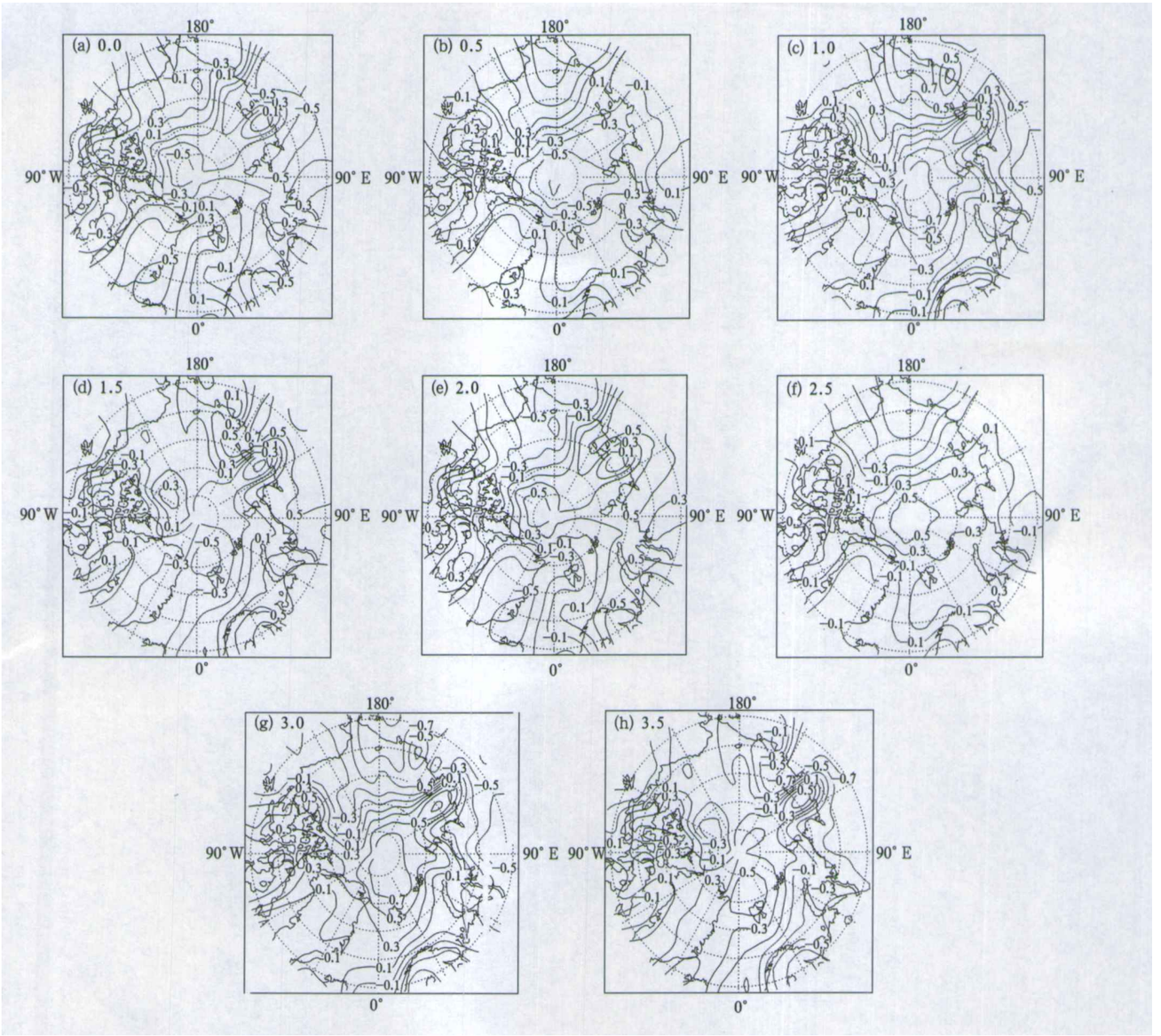

Fig.2. As in Fig.1, but for surface air temperature (SAT).

anomaly here is the same as that in the region near North America within the Arctic Ocean. The variation of SST anomaly here is connected with different phases of NAO.

In the model, the variation of SIC is determined by SST. When SST is above the freezing point, sea ice gets heat flux from water and SIC is reduced by melting laterally. When SST is below the freezing point, new ice forms and SIC grows. Once ice mass changes, through absorbing or releasing latent heat fluxes, SST variation is affected. In the inner part of the Arctic Ocean, accompanying with the anticlockwise propagation of positive and negative anomalies of SST, the negative and positive anomalies of SIC move anticlockwise (figure omitted). In the Greenland Sea and Barents Sea, connected with the quasi-stationary oscillation of SST anomaly, SIC anomaly oscillates quasi-stationarily.

3.3 Interannual cycle in SHF at the atmosphere-ocean interface

Figure 4 is for the composites corresponding to eight phases of reconstructed SHF, in which negative and positive values mean above and below the normal

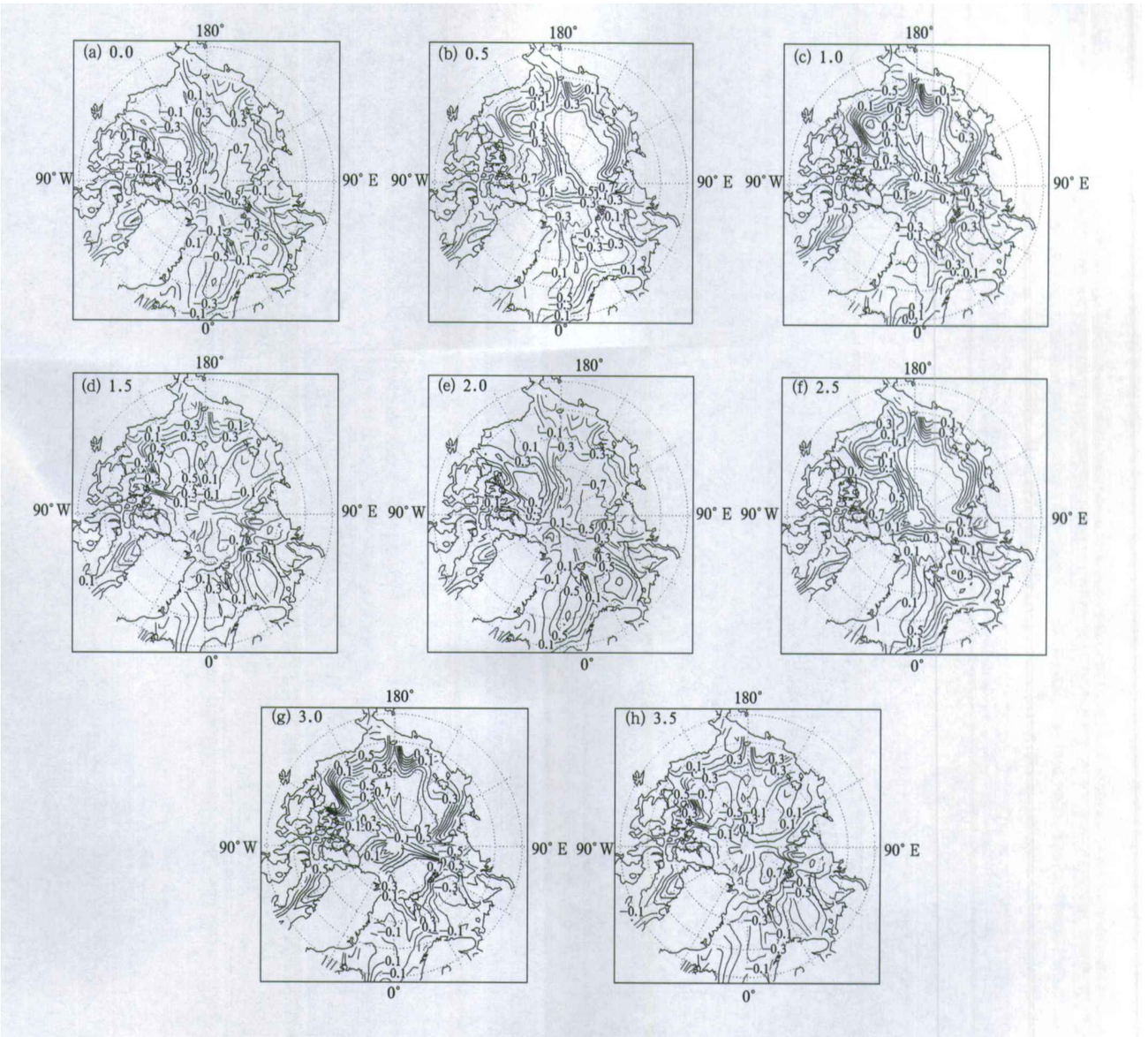

Fig.3. As in Fig.1, but for sea surface temperature (SST).

supply of SHF from the ocean to the atmosphere respectively. Within the Arctic Ocean, there is an inverse tendency between SHF anomaly near the Beaufort Sea and the Chukchi Sea and that in other regions. This is due to the variation of atmospheric circulation. When SAT is higher than normal, the ocean releases less SHF to the atmosphere, and vice versa. During the 0th–1.5th year, the SHF sent to the atmosphere is less than normal in the region near the Beaufort Sea and the Chukchi Sea, whereas during the 2nd–3.5th year, the SHF sent to the atmosphere is more than normal. In the 0th year, the SHF sent to the atmosphere is more than normal in the Barents Sea and less than normal in the Greenland Sea and the Norway Sea. Later, the area above the normal release of SHF in the Barents Sea extends towards the Greenland Sea and the Norway Sea. In the 2nd year, the Greenland Sea and the Norway Sea are totally covered by anomalies of above-normal release of SHF and the Barents Sea has been partly covered by anomalies of below-normal release of SHF. Afterwards, the area below the normal release of SHF begins to extend and in the 3.5th year it has covered the Greenland Sea and the Norway Sea totally. Meanwhile, the anomaly of SHF release has changed to the above-normal in part of the Barents Sea. Then, a new cycle repeats. The variation of SHF

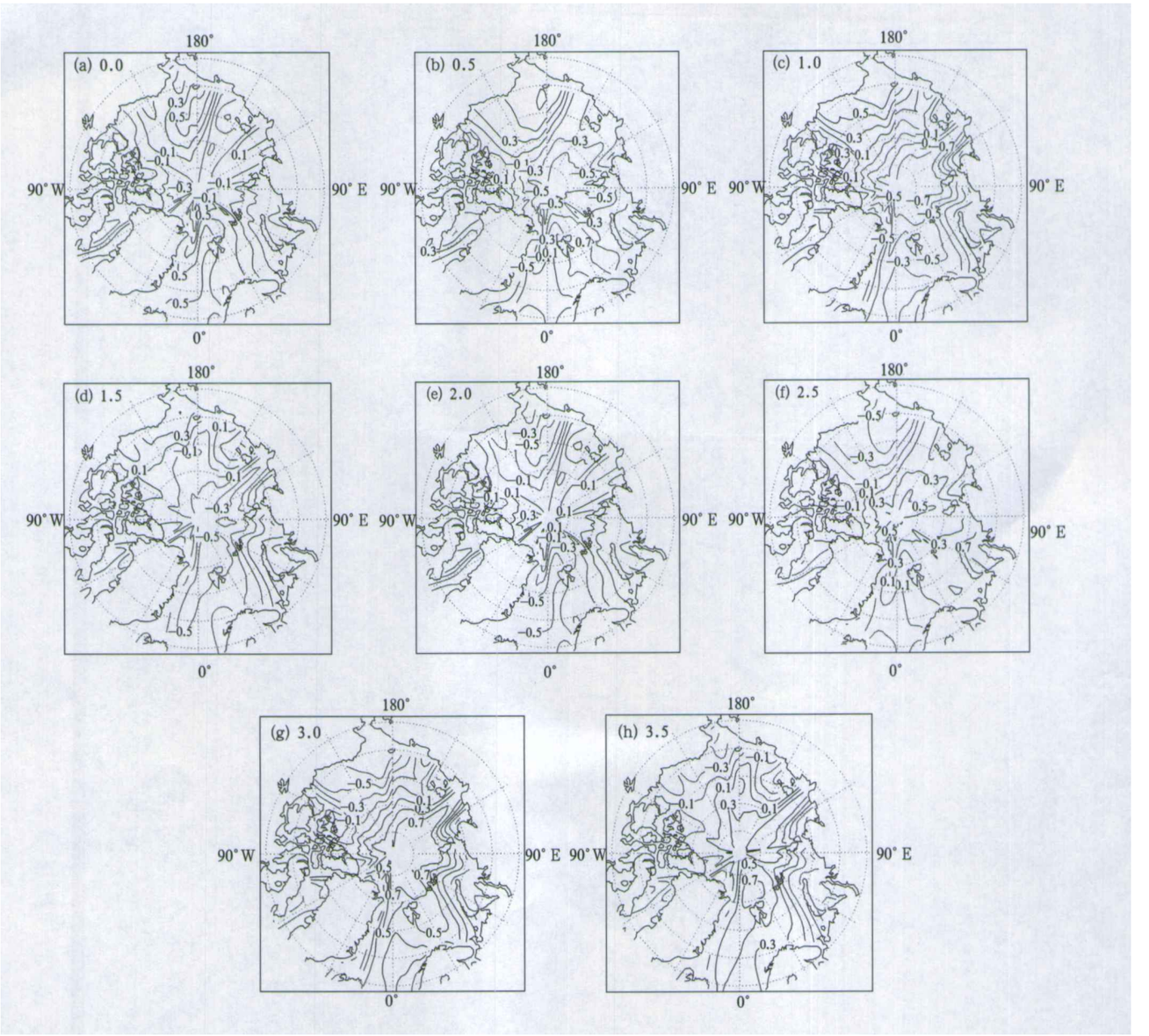

Fig.4. As in Fig.1, but for sea surface sensible heat flux (SHF).

anomaly sent to the atmosphere from the ocean is mainly controlled by the atmospheric general circulation since the pace of SHF variation is consistent with that of SAT.

3.4 Features of AOSI during an interannual cycle

The variation features during the interannual cycle of physical fields representing the atmosphere, ocean, sea ice, and atmosphere-ocean exchange have been discussed in the previous sections. In this section, relationships between these variations of physical variables will be analyzed and then features of AOSI during interannual cycle will be investigated. Since features of interaction may be region-dependent, the analysis will be performed for each region separately.

3.4.1 The Greenland Sea and the Barents Sea

From Figs.1–4, when NAO is in its positive phase (2.5th year), the southerly anomaly appears in the Greenland Sea, SAT increases, the sea loses less SHF, the warm current of the North Atlantic Ocean strengthens, SST increases, and SIC decreases accordingly; when NAO is in its negative phase (0.5th year), the northerly anomaly appears in the Greenland Sea,

SAT decreases, the sea loses more SHF, the warm current of the North Atlantic Ocean weakens, SST decreases, and SIC increases accordingly. The features of variation in the Barents Sea are similar to that in the Greenland Sea with temporal evolution, not totally identical.

3.4.2 Region within the Arctic Ocean

From results of former analysis, it can be seen that, on an average of multiple years, the area near the pole within the Arctic Ocean is a cold center. When the inner part of the Arctic Ocean is covered with a low pressure anomaly (during the 1st and 1.5th year), which is biased toward the Pacific Ocean, there is a warm advection anomaly in the region within the Arctic Ocean near the Pacific Ocean and a cold advection anomaly in the region within the Arctic Ocean near the Atlantic Ocean. Accompanying with the anomalies of warm and cold advection, warm and cold anomalies emerge in the two regions respectively. Meanwhile, the amount of SHF sent to the atmosphere is below and above normal respectively, the SST is in positive and negative anomalies respectively and the SIC is in negative and positive anomalies respectively. When the inner part of the Arctic Ocean is covered with high pressure anomaly (during the 3rd and 3.5th year), the situation is reversed. Therefore, the variations of SST and SIC are regulated by that of atmospheric general circulation.

3.4.3 Other regions

There is no ice in the Bering Sea, Okhotsk, or Labrador Seas in summer half year. With the performing of data processing with filter on SIC, noises introduced could have great influence on results of analysis. Thus no analysis is made for that region. Since the area of Baffin Bay is small and simulation results of ocean model there may be hampered by boundary conditions, no analysis is made for that region either.

4. Conclusions and discussions

By analyzing simulation results of a global atmosphere-ocean-sea ice coupled model, the interannual AOSI in high northern latitudes is studied. Five physical fields, SLP, SAT, SST, SIC, and SHF representing the state of the atmosphere, ocean and their interactions are filtered with a digital filter at first. Then the filtered fields are normalized and then used to perform the decomposition of CCEOF. At last, the five physical fields are reconstructed with the leading mode from the decomposition results. The features of variation during a periodical cycle (approximately 4 yr) in the atmosphere, ocean and their interactions represented by the five reconstructed fields in high northern latitudes are analyzed. The relationships between them are further inspected and features of AOSI during the periodical cycle in the Greenland Sea, Barents Sea, and the Arctic Ocean regions are analyzed. It is shown that, during the periodical cycle in the atmosphere and ocean, the variation of large-scale atmospheric general circulation plays a dominant role and variations of SST are mainly responding to it. The effects of change of atmospheric general circulation are deployed by influencing exchange of heat flux between the atmosphere and oceans (including sea ice) through anomalies of SAT and surface wind. On relationship between ocean and sea ice, the variations of SST determines that of SIC for the most part whereas variation of sea ice mass can resist SST change to some extent through the release or absorption of latent heat from phase transition. On relationship between atmosphere and sea ice, the direction changes of SHF transportation are mainly determined by variations of atmospheric general circulation and effects of SIC on variation of SHF for a model horizontal grid is comparatively small, which contribute to the result that the variation of SIC is responding to that of atmospheric general circulation. These results agree with those of research on dataset from observation (Slonosky et al., 1997; Wu et al., 2000).

There are two ways that atmospheric general circulation can influence sea ice variation, of which, one is through affecting temperature advection to drive sea ice to grow or wither away thermodynamically, and the other is through direct driving sea ice motion dynamically. It has been noted that the outflow of sea ice masses through Fram Strait has important impact on variations of sea ice in the Greenland Sea (Vinje, 2001) and the amount of outflow flux is modulated by Dipole anomaly in the winter arctic atmosphere (Wu

et al., 2006). It should be noted that the sea ice model used here excludes dynamic processes. Hence the interaction of ocean-sea ice and atmosphere-sea ice deployed in the model are nearly pure thermodynamic in high northern latitudes. If the effects of divergence and convergence of sea ice on AOSI due to dynamic processes are considered, then new features might be disclosed.

REFERENCES

Agnew, T., 1993: Simultaneous winter sea-ice and atmospheric circulation anomaly patterns. *Atmos. Ocean*, **31**, 259–280.

Barnet, T. P., 1983: Interaction of the monsoon and Pacific trade wind system at interannual time scale. Part I: the equatorial zone. *Mon. Weather Rev.*, **111**, 756–773.

Deser, C., J. E. Walsh, and M. S. Timlin, 2000: Arctic sea ice variability in the context of recent atmospheric circulation trends. *J. Clim.*, **13**, 617–633.

Gao Dengyi and Wu Bingyi, 1998: Preliminary study on decadal oscillation and its oscillation source of the sea-ice-air system in the Northern Hemisphere. *Scientia Atmospherica Sinica*, **22**, 137–143. (in Chinese)

Grotzner, A., R. Sausen, and M. Claussen, 1996: The impact of sub-grid scale sea-ice inhomogeneities on the performance of the atmospheric general circulation model ECHAM. *Clim. Dyn.*, **12**, 477–496.

Honda, M., K. Yamazaki, H. Nakamura, and K. Takeuchi, 1999: Dynamic and thermodynamic characteristics of atmospheric response to anomalous sea ice extent in the sea of Okhotsk. *J. Clim.*, **12**, 3347–3358.

Horel, J. D., 1984: Complex principal component analysis: theory and examples. *J. Clim. Appl. Meteor.*, **23**, 1660–1673.

Huang Shisong, Yang Xiuqun, and Xie Qian, 1992: Observational analysis and numerical study on the effect of the northern pole ice on the atmospheric general circulation and climate. *Acta Oceanologica Sinica*, **14**, 30–46. (in Chinese)

Jiang Quanrong, Wang Chunhong, and Xu Guiyu, 1996: Variation of the arctic sea ice cover in region I and its relation to the atmospheric teleconnection patterns. *Acta Meteor. Sinica*, **54**, 240–246. (in Chinese)

Jin Xiangze, Zhang Xuehong, and Zhou Tianjun, 1999: Fundamental framework and experiments of the third generation of IAP/LASG world ocean general circulation model. *Adv. Atmos. Sci.*, **16**, 197–215.

Liu Qinzheng, Huang Jiayou, Bai Shan, and Wu Huiding, 2000: Global simulation of sea ice with a coupled ice-ocean model. *Earth Science Frontiers*, **7**, 219–228. (in Chinese)

Liu Xiying, Zhang Xuehong, Yu Yongqiang, and Yu Rucong, 2004: Coupling of atmospheric general circulation model with oceanic general circulation model under sub-grid scale sea ice inhomogenities. *Plateau Meteorology*, **23**, 344–347. (in Chinese)

Liu Xiying, Zhang Xuehong, Yu Rucong, and Yu Yongqiang, 2005: A case study of interannual anomaly of sea ice variation in Greenland Sea in an ocean-sea ice-atmosphere coupled model. *Chinese Journal of Atmospheric Sciences*, **29**, 795–804. (in Chinese)

Ni Yunqi, Zhang Qi, and Li Yuedong, 1992: A numerical study for mechanism of the effect of north summer Arctic ice cover on the global short-range climate. *Acta Meteor. Sinica*, **6**, 15–24.

Parkinson, C. L., and W. M. Washington, 1979: A large-scale numerical model of sea ice. *J. Geophys. Res.*, **84**, 311–337.

Semtner, Jr. A. J., 1976: A model for the thermodynamic growth of sea ice in numerical investigations of climate. *J. Geophys. Res.*, **6**, 379–389.

Slonosky, V. C., L. A. Mysak, and J. Derome, 1997: Linking Arctic sea ice and atmospheric circulation anomalies on interannual and decadal time scales. *Atmos. Ocean*, **35**, 333–366.

Vinje, T., 2001: Fram strait ice fluxes and atmospheric circulation: 1950–2000. *J. Clim.*, **14**, 3508–3517.

Wu Bingyi, Huang Ronghui, and Gao Dengyi, 2000: Arctic sea ice bordering on the North Atlantic and interannual climate variations. *Chinese Sci. Bull.*, **45**, 1993–1997. (in Chinese)

Wu B. Y., Wang J., and J. E. Walsh, 2006: Dipole anomaly in the winter arctic atmosphere and its association with sea ice motion. *J. Clim.*, **19**, 210–225.

Ye Zhengqing, Dong Min, and Chen Jiabin, 2000: Simulated climate by National Climate Center GCM with the observed SST. *Development of Dynamical Model System for Short-Term Climate Prediction in China*, Ding et al., Eds. China Meteorological Press, Beijing, 70–89. (in Chinese)

Yu Yongqiang and Zhang Xuehong, 2000: Schemes for coupling AGCM and OGCM. *IAP Global Ocean-Atmosphere-Land System Model.* Zhang Xuehong, Shi Guangyu, Liu Hui et al., Eds. Science Press, Beijing, 100–112.

Zhang Xuehong, Chen Keming, Jin Xiangze, et al., 1996: Simulation of the thermohaline circulation with a twenty-layer oceanic general circulatoin model. *Theoretical and Applied Climatology*, **55**, 65–87.